Science and Technology Indonesia
e-ISSN:2580-4391 *p*-ISSN:2580-4405
Vol. 11, No. 2, April 2026

Research Paper

Heterocyclic Azo Compounds, Synthesis, Characterization, Evaluation as Antimicrobial, and Theoretical Study

Mohammed K. Mohammed[1*], Afrah A. Al-Jaber[2], Rafid H. Al-Asadi[1], Hawraa K. Dhaef[1]

[1]*Department of Chemistry, College of Education for Pure Sciences, University of Basrah, Basrah, 61004, Iraq*
[2]*Education Directorate of Basrah, Ministry of Education, Basrah, 61004, Iraq*
***Corresponding author**: mohammed.khalaf@uobasrah.edu.iq

Abstract
Five azo compounds, including N-(3-hydroxyphenyl) maleimide, were synthesized and characterized using FT-IR, ^{1}H-NMR, ^{13}C-NMR, and mass spectroscopy. The compounds were evaluated for antibacterial activity against *Staphylococcus aureus* and *Pseudomonas aeruginosa* using the disk diffusion method. The screening results showed that the azo compounds tested were effective against the bacteria tested, particularly *Staphylococcus aureus*. The geometry optimization of the molecular structures and the energy calculations for compounds 1-5 were performed using the density functional approach. Molecular docking was conducted to examine the interaction of the synthesized compound 1 with two bacterial receptors and one viral receptor (neuraminidase). It was found that they would target the PDB:4CJN protein, for which the compound yielded the lowest binding energy.

Keywords
Azo Compounds, Antimicrobial, DFT, Molecular Docking

Received: , Accepted:
https://doi.org/10.26554/sti.2026.11.2.

1. INTRODUCTION

One of the most significant challenges in modern medicine is the rapid emergence of antimicrobial resistance (AMR) (Upadhayay et al., 2023), which is increasingly making it difficult to treat diseases with conventional antibiotics (Upadhayay et al., 2023; Adu et al., 2020). The adaptability of pathogenic bacteria to develop resistance through processes like enzymatic inactivation, efflux, and target modulation has created a need to design new antimicrobial agents that act through different mechanisms (Hamdani et al., 2020).

Heterocyclic compounds have received widespread attention in medicinal chemistry owing to their diverse structures (Irminova et al., 2020; Scarim and Chin, 2021), tunable electronic properties, and a wide range of pharmacological activities (Jarallah et al., 2026; Shafeeq et al., 2023). Of interest are the azo compounds (−N=N–) (Rabel and Prabhath, 2015), which exhibit distinctive redox properties, π-electron conjugation systems, and the ability to bind to biomolecules such as enzymes and nucleic acids (Jasim et al., 2023; Widjajanti et al., 2021). A number of azo compounds have been found to possess antibacterial, antifungal, antioxidant, anticancer, and enzyme inhibitory properties (Marinescu et al., 2022; Mohammed et al., 2024).

The incorporation of heterocyclic rings into azo structures further enhances biological activity by increasing stiffness and lipophilicity and by enhancing binding affinity for biological targets (Piotto et al., 2017; Shafeeq et al., 2023). In particular, maleimide scaffolds are well known for their electrophilic character, which can engage in either covalent or noncovalent interactions with nucleophilic amino acid side chains in enzymes/proteins. This makes them highly suitable for applications in antimicrobial agents (Dhaef et al., 2021; Mutlaq et al., 2021). The presence of additional functional groups, such as nitro, sulfonamide, thiazole, or benzothiazole rings, will help modulate biological properties.

Although extensive work has examined azo dyes and maleim ide compounds, research on heterocyclic azo compounds and maleimide cores to study their antibacterial properties, both experimentally and theoretically, remains limited. Additionally, research on the correlation between molecular structure and electronic properties (HOMO-LUMO gap and dipole moment) and biological activity is limited. Furthermore, the use of docking analysis against bacterial penicillin-binding proteins and viral enzymes has not been explored to a great extent for these compounds.

As such, this study seeks to develop a novel series of heterocyclic azo compounds from N-(3-hydroxyphenyl)maleimide and to assess their antibacterial activity against selected Gram-

positive and Gram-negative bacterial strains. To further elucidate structure-activity relationships and to provide insight into possible molecular-level interactions, density functional theory DFT calculations and molecular docking analyses were also employed. This approach, which combines experimental and theoretical components, will provide deeper insight into the antimicrobial activity of heterocyclic azo compounds and inform the design of novel antimicrobials.

2. EXPERIMENTAL SECTION

2.1 Materials

Materials. Various companies, including Sigma-Aldrich and Alpha, supplied all chemicals and solvents used in this work. All synthesized compounds were evaluated for biological activity at the University of Tarbiyat Modarres, Iran. NMR spectra were recorded on a Bruker inovo AV-400 spectrometer (Germany) at room temperature, using DMSO-D_6 as the solvent, to obtain ^{1}H and ^{13}C spectra at the University of Basrah, College of Education for Pure Science. The coupling constant (J) and chemical shifts (δ scale) were measured in hertz (Hz) and parts per million (ppm), respectively. The precise mass of the synthesized compounds is determined using a micro-mass LCT apparatus in electrospray ionization (ESI) mode (Iran). Bioactivity was conducted at the Medicinal Plants and Drugs Research Institute of Shahid Beheshti University in Iran. To weigh the samples, a D225CPA model manufactured by Sartorius AG (Göttingen, Germany) was used. The incubator used in this test is an Incubator model D-63450, manufactured by Heraeus (Hanau, Germany).

2.2 Methods

2.2.1 Preparation of N-(3-Hydroxyphenyl) Maleimide (Morrison et al., 2019)

At room temperature, in a conical flask, 3.50 g of 3- aminop henol was mixed with 3.80 g of maleic anhydride in 10 mL of dimethylformamide (DMF). The mixture was stirred for 2 hours to produce a maleamic acid derivative. A mixture of 1.85 g of phosphorus pentoxide and 480 μL of concentrated sulfuric acid in 15 mL of dimethylformamide was slowly added to most of the reaction mixture over a period of one hour. The resultant mixture was agitated at 80°C for 5 hours, then cooled to ambient temperature and transferred to 250 mL of cold water. The solid that formed was collected, cleaned with isopropanol, and dried in a vacuum to produce N-(3-hydroxyphenyl) maleimide as a yellow solid. Produce 2.8 g (40%), m.p. 125-128°C

2.2.2 Synthesis of Heterocyclic Azo Compound Derivatives

4-methyl-3-nitroaniline (0.01 mol) was combined with water (3 mL) and conc. HCl (3 mL), then cooled to 5°C using an ice bath. A solution of $NaNO_2$ was prepared by dissolving 0.01 mol in 10 mL of water. Next, the sodium nitrate solution was slowly mixed into the 4-methyl-3-nitroaniline solution at 5°C while stirring. The mixture was then slowly added to a solution of N-(3-hydroxyphenyl)maleimide (1.89 g, 0.01 mol) in 20 mL of 10% NaOH at 5°C. The solution was maintained at a low temperature in an ice bath and continuously agitated for 10 minutes. The solid was filtered, purified with glacial acetic acid, rinsed with methanol, and then dried in an oven at 65°C for 24 hours to afford compound 1. Other compounds were prepared in the same way, using the appropriate amine. All synthesized compounds 1-5 were of purity more than 90%.

(E)-1-(3-hydroxy-4-((4-methyl-3-nitrophenyl) diazenyl) phenyl)-1H-pyrrole-2,5-dione (1). A dark-orange powder, yield: 63%; m.p. 191-193 °C; IR (KBr) cm^{-1}, ν: 2900-3370 (OH), 3197 (CH, CH=CH), 3070 (CH aromatic), 1701 (C=O), 1458-1610 (N=N, C=C) azo, olefin, and phenyl, respectively. ^{1}H NMR (DMSO-d_6) δ (ppm): 2.58 (s, 3H, CH_3), 6.44 (d, 1H, J = 12 Hz, CH=CH), 6.65 (d, 1H, J = 12 Hz, CH=CH), 7.67–8.47 (m, 6H aromatiques), 10.44 (s, 1H, OH). ^{13}C NMR (DMSO-d_6) δ/ppm: 19.83, 108.13, 112.84, 118.38, 119.62, 127.42, 131.98, 133.51, 134.2, 134.58, 134.75, 139.46, 149.93, 151.20, 163.77, 167.88. MS (EI) m/z = 352.31 [M+1]$^+$.

(E)-1-(4-((4,5-dihydrothiazol-2-yl) diazenyl)-3- hydroxyp henyl)-1H-pyrrole-2,5-dione (2). A dark-brown powder, yield of 53%; m.p. 175-176 °C; IR (KBr) cm^{-1}, ν: 2800-3400 (OH), 3113 (CH, CH=CH), (CH aromatic overlap with OH peak), 1701–1716 (C=O), 1419–1606 (N=N, C=C, C=C) olefine, phenyl, and azo respectively. ^{1}H NMR (DMSO-d_6) δ/ppm: 6.39 (d, 1H, J = 12 Hz, CH=CH), 6.25 (d, 1H, J = 12 Hz, CH=CH), 7.76-7.85 (m, 3H aromatic), 10.49 (s, 1H, OH). ^{13}C NMR (DMSO-d_6) δ/ppm: 108.24, 113.60, 120.57, 122.55, 130.76, 132.66, 134.28, 139.83, 144.11, 163.82, 167.46. MS (EI) m/z = 302.31 [M+H]$^+$.

(E)-1-(4-((4-acetylphenyl)diazenyl)-3-hydroxyphenyl)-1H -pyrrole-2,5-dione (3). A dark-brown powder, yield: 70%; mp 179-181 °C; IR (KBr) cm^{-1}, ν: 2800-3360 (OH), 1714-1701 (C=O ketone, C=O amide respectively) (CH=CH, CH aromatic overlap with O−H peak), 1508-1608 (N=N azo, C=C alkene, C=C phenyl ring). ^{1}H NMR (DMSO-d_6) δ/ppm: 2.63 (s, 3H, CH_3), 6.41 (d, 1H, J = 12 Hz, CH=CH), 6.68 (d, 1H, J = 12 Hz, CH=CH), 7.75-8.14 (m, 7H aromatic), 10.69 (s, 1H, OH). ^{13}C NMR (DMSO-d_6) δ/ppm: 27.42, 108.06, 112.88, 120.08, 123.22, 129.89, 131.01, 132.37, 134.92, 137.94, 139.42, 155.12, 163.82, 167.79, 197.89. MS (EI) m/z = 335.12 [M+H]$^+$.

(E)-4-((4-(2,5-dioxo-2,5-dihydro-1H-pyrrol-1-yl) -2-hyd roxyphenyl) diazenyl) benzenesulfonamide (4). A darg-orang powder, yield: 53%; mp dec. at 259 °C; IR (KBr) cm^{-1}, ν: 2900-3300 (OH), 3342 NH_2, 1710 C=O amide, (CH=CH, CH aromatic overlap with O−H peak), 1468-1610 (N=N azo, C=C alkene, C=C phenyl ring). ^{1}H NMR (DMSO-d_6) δ/ppm: 6.40 (d, 1H, J = 12 Hz, CH=CH), 6.68 (d, 1H, J = 12 Hz, CH=CH), 7.38 (s, 2H, NH_2), 7.55-8.23 (m, d, d, 7H, Haromatic), 10.47. ^{13}C NMR (DMSO-d_6) δ/ppm: 111.06, 116.88, 123.78, 126.22, 132.89, 133.31, 135.73, 142.74, 143.42, 158.12, 167.91, 168.12. MS (EI) m/z = 372.36 [M+H]$^+$.

(E)-1-(4-(benzo[d]thiazol-2-yldiazenyl)-3-hydroxyphenyl)-

1H
-pyrrole-2,5-dione (5). A brown powder, yield: 73%; mp 186-187 °C; IR (KBr) cm^{-1}, ν: 3000–3200 (OH), 3120 (CHvinyl) (CHaromatic overlapping with OH band), 1672 (C=O), 1467-1610 (N=N azo, C=C vinyl, C=C aromtic, respectively). ^{1}H NMR (DMSO-d_6) δ/ppm: 6.41 (d, 1H, J = 12 Hz, CH=CH), 6.68 (d, 1H, J = 12 Hz, CH=CH), 7.52-8.10 (m, 9H aromatic), 10.68 (s, 1H, OH). ^{13}C NMR (DMSO-d_6) δ/ppm: 108.04, 112.87, 119.85, 123.48, 127.28, 130.96, 132.38, 134.80, 139.49, 145.37, 154.23, 163.78, 176.81. MS (EI) m/z = 350.35 $[M+H]^+$.

2.2.3 Antimicrobial assay

Two bacterial strains (*E. coli* and *S. aureus*) were selected for antibacterial activity. The CLSI method was used for testing (Standard test) (Wiegand et al., 2008). The microbial strains were characterized by growing them on nutrient agar. Twelve different concentrations for each sample were used in this test (2.5, 1.25, 0.625, 0.312, 0.156, 0.078, 0.039, 0.0195, 0.0097, 0.0048, 0.0024, and 0.0012 mM). The bacterial suspension used contained 106 CFU/mL. Mueller-Hinton broth (Condalab (Madrid, Spain)) culture medium was used for the MIC test, and Nutrient broth (Condalab (Madrid, Spain)) culture medium was used for the MBC test. A stock solution a 20 mM was prepared for all samples. 160 µL of culture medium was poured into the first well. 100 μL of culture medium was poured into the remaining wells. 40μL of the sample dissolved in DMSO was poured into the first well. Then 100 μL was transferred from the first well to the second, and then from the second to the third. This work was performed up to well 12, and 100 μL was then removed from well 12 and discarded, so that all wells had a volume of 100 μL.

2.2.4 Computational Study

The shapes and energy levels of compounds 1-5 can be determined using density functional theory (DFT), employing the BLYP functional and the standard DNP basis set in Materials Studio-DMol3 Version 2017. A molecular docking analysis of molecule 1 was carried out using MOE 2019. First, the Ligand molecule (Compound 1) is drawn, geometrically optimized until it reaches the lowest energy, and then saved as a PDB file. The second stage is the preparation of the protein molecule, in which the 3D structure is downloaded from the Protein Data Bank website https://www.rcsb.org/structure and configured within the program by removing the excess water molecules and reattaching some broken bonds. In the third stage, the run docking simulation of the ligand molecule on the protein is run to determine the forms and types of associations that occur (Al-Asadi et al., 2020).

3. RESULTS AND DISCUSSION

3.1 Synthesis and Characterization

The heterocyclic azo compounds 1-5 were synthesized via a two-step procedure. Step 1 - Synthesis of N-(3-hydroxyphenyl) maleimide: Maleic anhydride was then reacted with 3-hydroxyaniline to give a Z-maleamic acid intermediate, which was then cyclized using a mixture of sulfuric acid and phosphorus pentoxide in dimethylformamide (DMF) to give N-(3-hydroxyphenyl). Step 2 - Synthesis of heterocyclic azo compounds: Diazonium salts were prepared from the corresponding aniline derivatives via diazotization brought about by sodium nitrite ($NaNO_2$) in the presence of hydrochloric acid at 0–5°C. A solution of N-(3-hydroxyphenyl)maleimide in a cold alkaline medium was then added dropwise to the diazonium salt solution. Thus, deprotonation of the hydroxyl group generated the phenoxide ion, which acted as the nucleophile, attacking the diazonium salts, thereby producing the desired heterocyclic azo compounds (1–5). The process is illustrated in Figure 1.

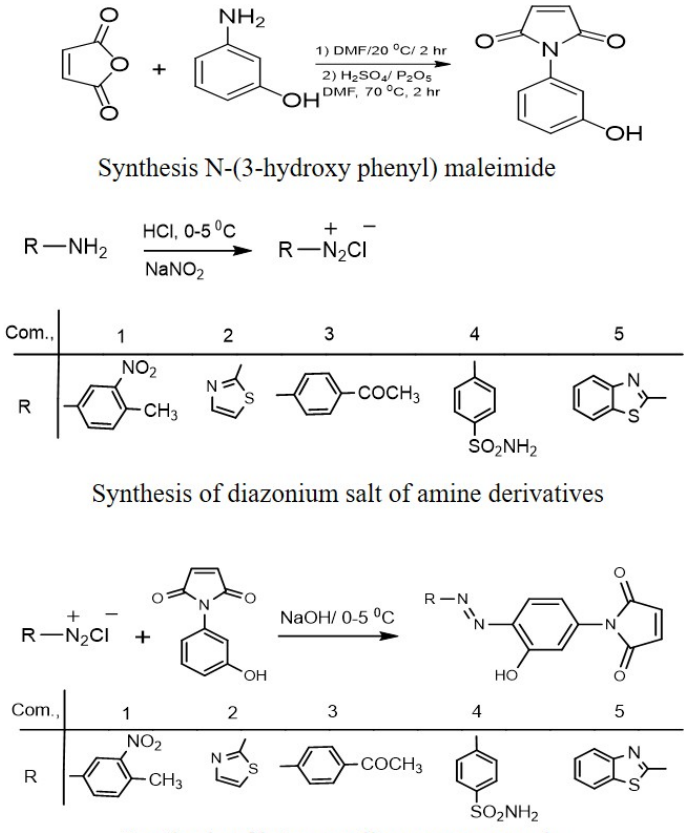

Figure 1. Synthesis Route of Heterocyclic Azo Compounds 1-5

The structures of the heterocyclic azo compounds 1-5 that have been synthesized have been confirmed using Fourier transform infrared spectra (FTIR), proton NMR spectroscopy (^{1}H NMR), carbon-13 NMR spectroscopy (^{13}C NMR), and mass spectra. From FT-IR, there was a prominent band around 1701 cm^{-1} in the spectra of compounds 1-5, which represented the carbonyl (C=O) stretching band in the maleimide ring. The bands corresponding to 3059–3120 cm^{-1} were associated with aromatic/vinylic C−H stretching, while those occurring in the range 1523-1610 cm^{-1} showed C=C stretching in aromatic and alkenes functional groups. The bands occurring in

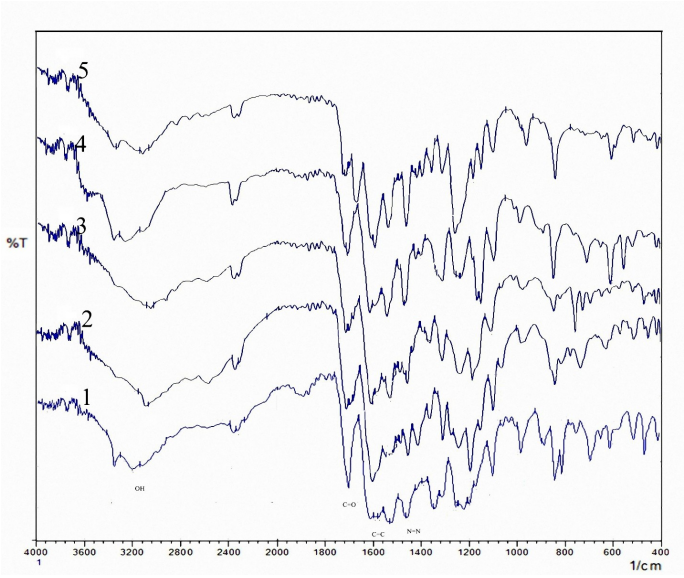

Figure 2. FT-IR Spectra of Compounds 1-5

the range 3380-3900 cm^{-1} were associated with O–H stretches. In comparison, the characteristic band for azo (N=N) was represented by a band occurring around 1460 cm^{-1}, which indicated successful azo bond formation (Figure 2).

In the ^{1}H NMR spectra, all the compounds showed two doublets between δ 6.30-6.70 ppm due to the maleimide vinylic protons. Compounds 1 and 3 showed a singlet signal at δ 2.58 and 2.63 ppm, respectively, due to the methyl protons. Aromatic proton signals occur between δ 7.00-8.00 ppm as expected by the presence of aromatic protons, and the downfield signal greater than δ 10.40 ppm was attributed to the phenolic OH proton. For compound 4, a broad NH_2 signal appeared around δ 7.38 ppm Figure 3.

These assignments were supported by ^{13}C NMR spectra with characteristic methyl carbons for compound 1 at δ 19.83 ppm and for compound 3 at δ 27.42 ppm, and numerous peaks in aromatic regions for phenyl rings bearing functional groups. Taken together, all data confirmed the proposals of structures for compounds 1-5 in Figure 4. Mass analysis by mass spectrometry for each compound yielded a distinct molecular ion peak corresponding to its calculated molecular mass, thereby confirming successful synthesis Figure 5.

3.2 Antibacterial Activity

The antibacterial activity of the synthesized heterocyclic azo dyes (1–5) was evaluated against *Staphylococcus aureus* (ATCC 12600, Gram-positive) and *Pseudomonas aeruginosa* (ATCC 27835, Gram-negative), as shown in Table 1. The synthesized compounds exhibited significant antibacterial activity, with greater inhibitory activity against *S. aureus* than against *E. coli*. This may be related to the natural resistance of Gram-negative bacteria to antimicrobial drugs, which cannot readily cross their outer membranes (Adu et al., 2020).

In the series, compound 1 had the most potent antibacterial activity with the lowest MIC values against both *S. aureus* (MIC = 0.125 μg/mL) and *E. coli* (MIC = 2 μg/mL). Compounds 2 and 3 were also highly effective as antibacterials, especially against *S. aureus* (MIC = 0.25 μg/mL), with good activity against *E. coli* (MIC = 1-2 μg/mL). By contrast, compounds 4 and 5 moderately inhibited bacterial growth, with an MIC of 1 μg/mL for *S. aureus* and 2 μg/mL for *E. coli*.

Since all compounds were synthesized from the same phenolic precursor, N-(3-hydroxyphenyl) maleimide, the differences in antibacterial activities could probably be ascribed to the nature of the amine-derived functional groups. Compound 1, which has nitro and methyl functional groups, had the highest antibacterial activity and indicated that electron-withdrawing functional groups could increase antibacterial activities. While compound 2, which has the thiazole structure, demonstrated antibacterial properties similar to those of compound 3, which has the acetophenone structure, the lower antibacterial activity of compounds 4 and 5 may be attributed to steric hindrance and reduced accessibility of the azo bond due to the sulfonamide and benzothiazole functional groups.

A comparative study of previously reported azo compounds, particularly those reported by Piotto et al. (2017), further supports the improvement in antibacterial activity achieved by the presented series. As can be reviewed in Table 1, the synthesized compounds show significantly lower MIC values against S. aureus (0.125-1 μg/mL) than the reported azo reference compounds, which showed an MIC of ≥2-32 μg/mL. Such improvements indicate the beneficial effect of combining the maleimide system with the heterocyclic azo moiety.

Structural and electronic factors account for the enhanced antibacterial activity. Unlike the relatively simple aromatic azo dyes documented in the literature, the compounds designed and synthesised here combine the conjugated azo bond with the maleimide ring system, thereby providing enhanced π-π stacking and hydrogen-bonding interactions with the bacterial enzyme. Moreover, the enhanced electron-withdrawing capability of the nitro/sulfonamide groups enables efficient electron distribution across the entire scaffold and, consequently, efficient interactions with target biological sites that contain the active residues. These findings are consistent with earlier reports on the structures and activities of nitro-substituted azo dyes (Jasim et al., 2023; Piotto et al., 2017).

Therefore, based on the results obtained in this comparison, it can be said that the synthesized azo-maleimide heterocyclic hybrids exhibit a marked superiority in their antimicrobial activity relative to the previously synthesized azo compounds. Additionally, the improved antimicrobial activity of compound 1 has been proven by density functional theory calculations and a molecular docking analysis.

3.3 DFT Study

Density functional theory (DFT) calculations were performed to optimize the geometries of compounds 1-5 and to investigate their electronic properties. The optimized molecular structure

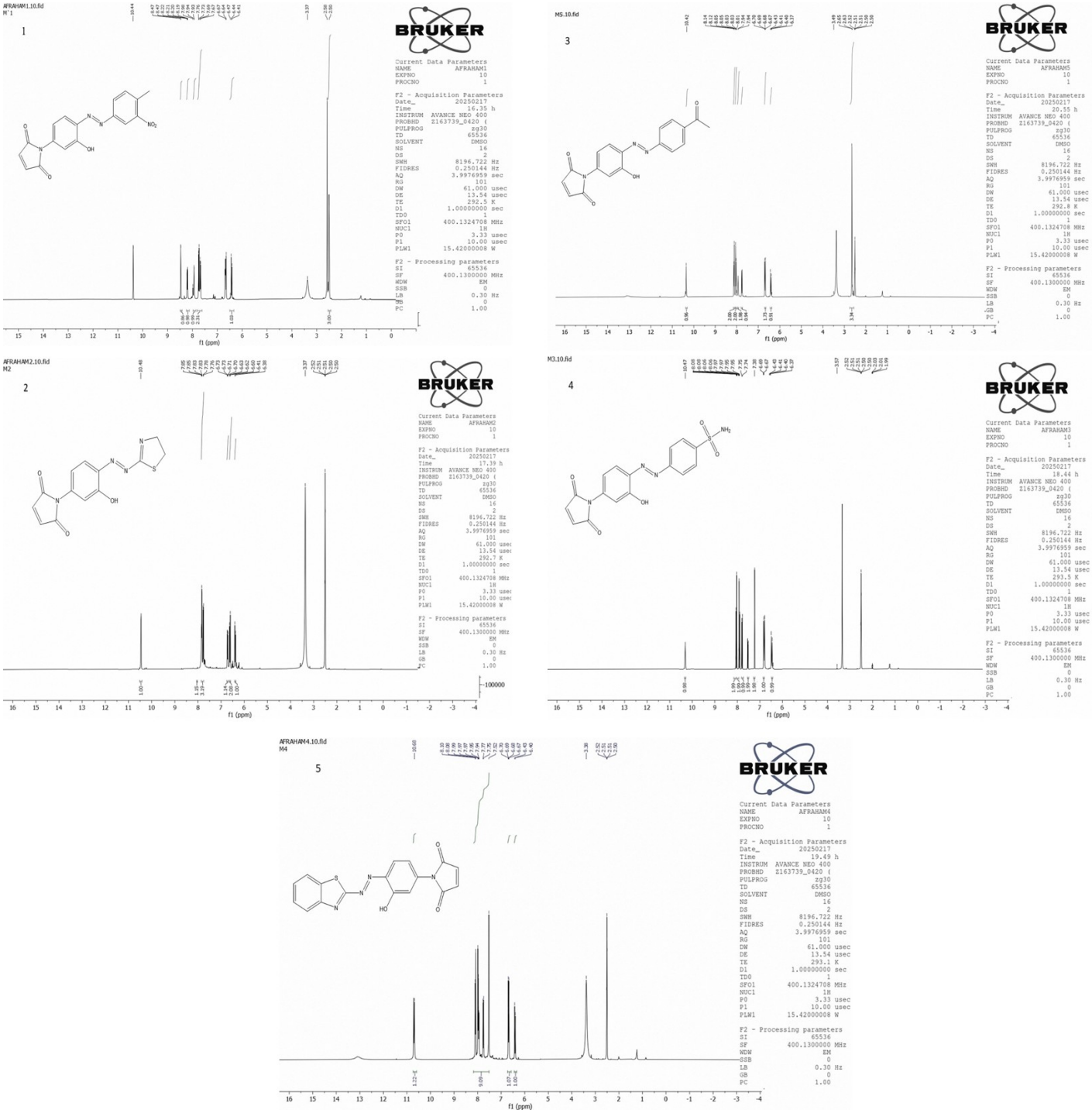

Figure 3. ^{1}H-NMR Spectra of Compounds 1-5

of the compounds is shown in Figure 6, and the data for the HOMO-LUMO energy gap (Δ EHOMO-LUMO), dipole moment, binding energy, and heat of formation are given in Table 2. These results provide information regarding the reactivity, stability, and biological activities of the synthesized compounds (Al-Asadi, 2019).

Among the compounds under investigation, compound 1 has the smallest HOMO-LUMO gap (1.030 eV) and the most significant dipole moment (7.437 Debye), making it more chemically reactive and more efficient in intermolecular interactions. A lower energy gap between the HOMO-LUMO is known to impart increased ability to transfer electrons, thus

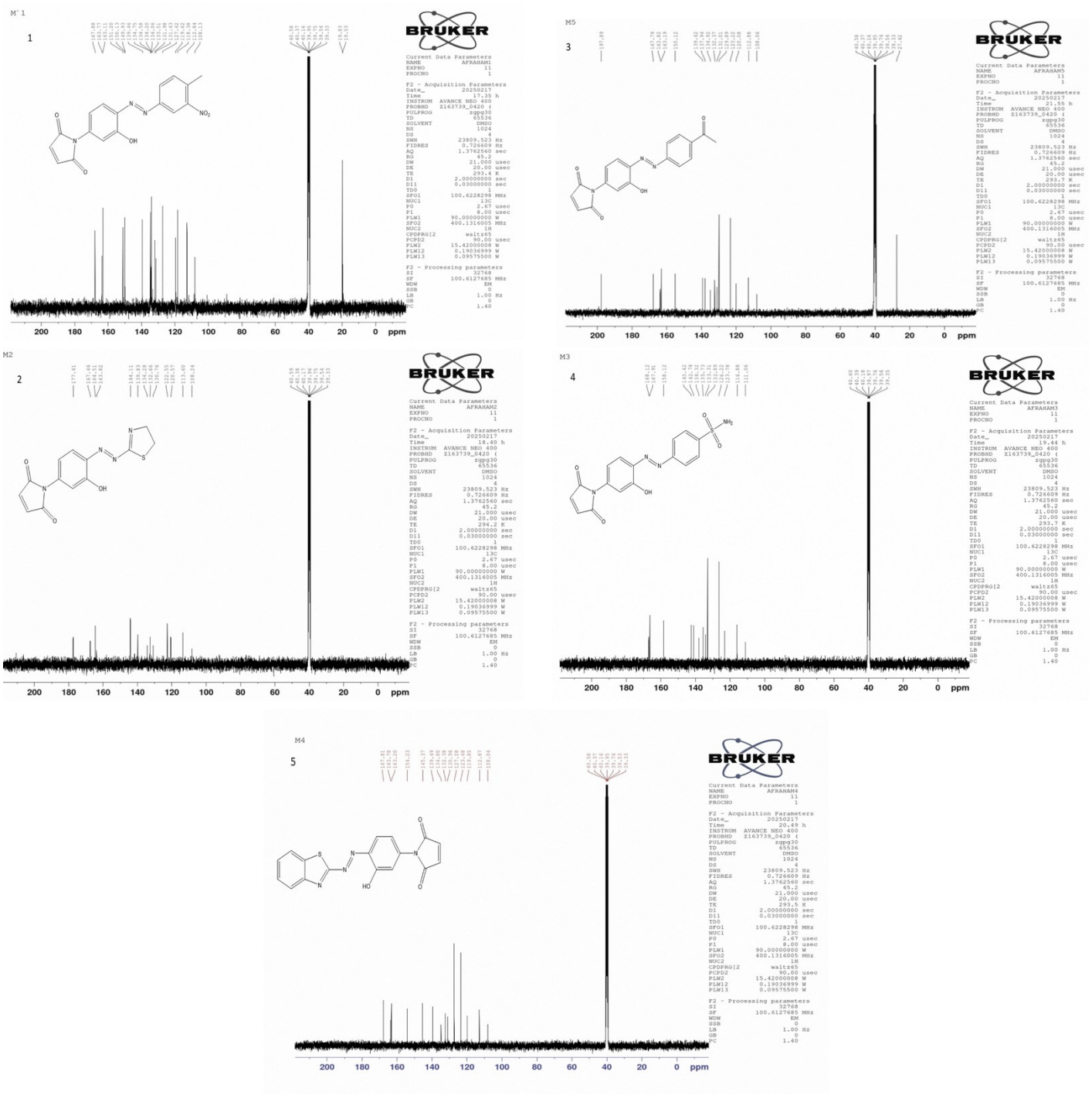

Figure 4. ^{13}C-NMR Spectra of Compounds 1-5

easily interacting with biological molecules, hence making a compound highly active biologically. Theoretical results are consistent with antibacterial experiments, in which compound 1 exhibited the highest biological activity among the synthesized compounds. The high chemical reactivity of compound 1 can be attributed to the presence of a conjugated azo and an electron-withdrawing nitro group, which readily delocalize electrons throughout the molecule.

The computed formation enthalpy and binding energies also confirm that all synthesized compounds are thermodynamically stable, thereby ensuring their successful isolation and characterization. Though the energy gaps of compounds 2 through 5 are larger compared to compound 1, they are in the range that indicates reasonable chemical reactivity and stability.

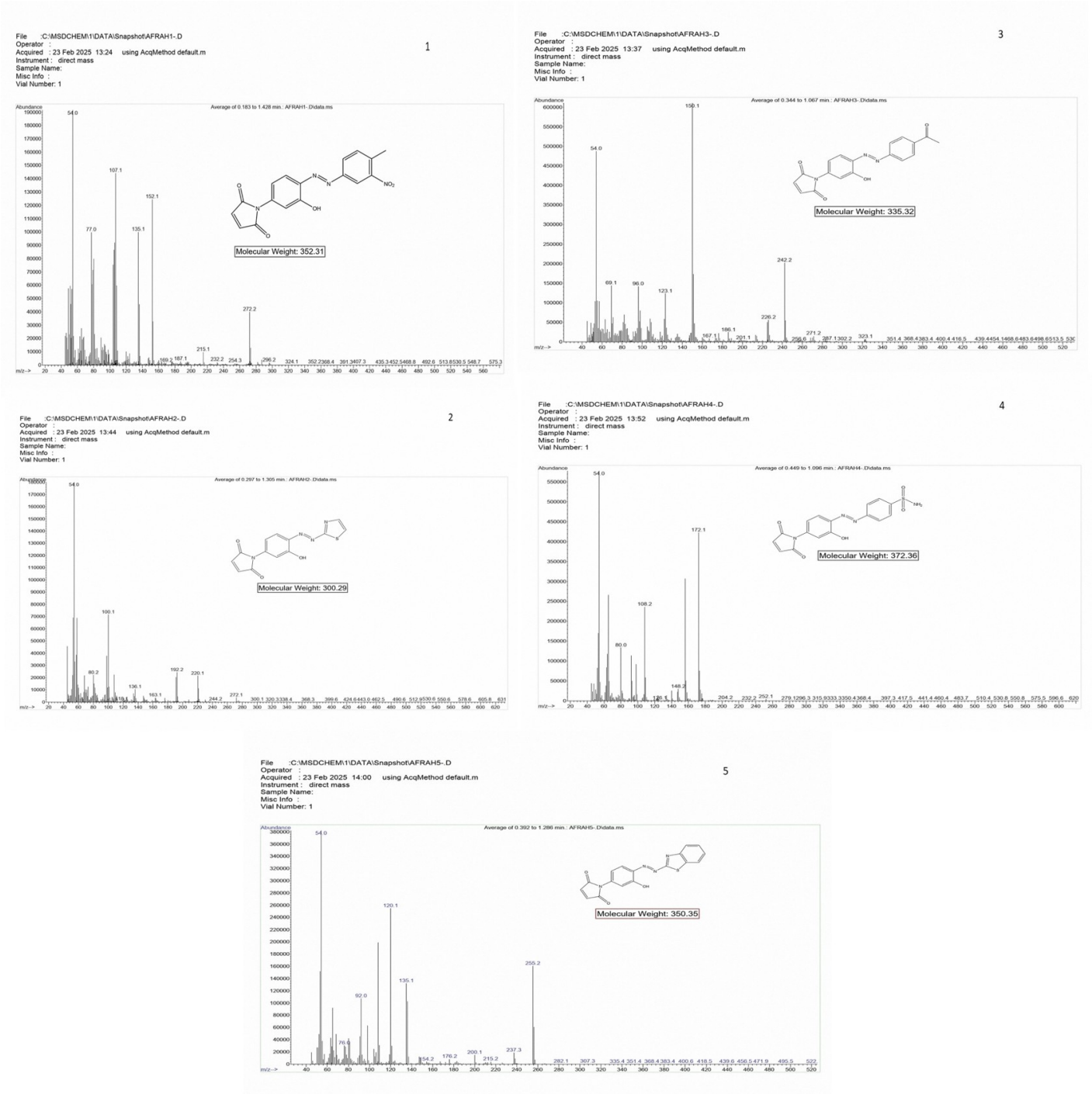

Figure 5. Mass Spectra of Synthesized Compounds 1-5

The molecular electrostatic potential maps and HOMO distributions of the compounds of interest have also been represented in Figure 7. The HOMO orbitals in these molecules are primarily localized on the azo bond and the aromatic rings of the neighboring systems, suggesting that these regions can serve as electron-donating sites. On the contrary, the molecular electrostatic potential maps highlight regions of high electron density around the azo nitrogens and the oxygen atoms of the hydroxyl and carbonyl groups in the molecules. Such areas serve as favorable sites for electrophilic attack and electrostatic interactions with amino acid moieties in biological molecules (Al-Ameertaha and Al-Asadi, 2025; Temma et al., 2025). In conclusion, the DFT results are consistent with the antibacterial activity of compound 1. This may be due to the low

Table 1. Antimicrobial Activity of Synthesized Compounds 1-5 Expressed as MIC (μg/mL), and Compared with Azo Compounds in Reference Piotto et al. (2017)

Sample	*S. aureus* ATCC12600		*E. coli* ATCC27835		Sample (Piotto et al., 2017)	
	MIC (mM)	MBC (mM)	MIC (mM)	MBC (mM)	*S. aureus* ATCC12600 MIC (mM)	*E. coli* ATCC27835 MIC (mM)
1	0.125	>2	2	>2	4a	32
2	0.25	>2	1	>2	4b	≥2
3	0.25	>2	2	>2	4c	>128
4	1	>2	2	>2	4d	4
5	1	>2	2	>2	4f	12

Table 2. Values of the Calculated Energies of the Studied Molecules

Molecules	HOMO Energy (eV)	HUMO Energy (eV)	$\Delta E_{\text{LUMO-HOMO}}$ (eV)	Dipole Moment (Debye)	Binding Energy (eV)
1	-4.953	-3.923	1.030	7.437	-8.672
2	-5.208	-3.830	1.378	1.184	-5.700
3	-5.324	-3.731	1.593	3.555	-7.293
4	-5.462	-3.765	1.697	6.450	-7.023
5	-5.389	-3.821	1.568	1.1222	-6.790

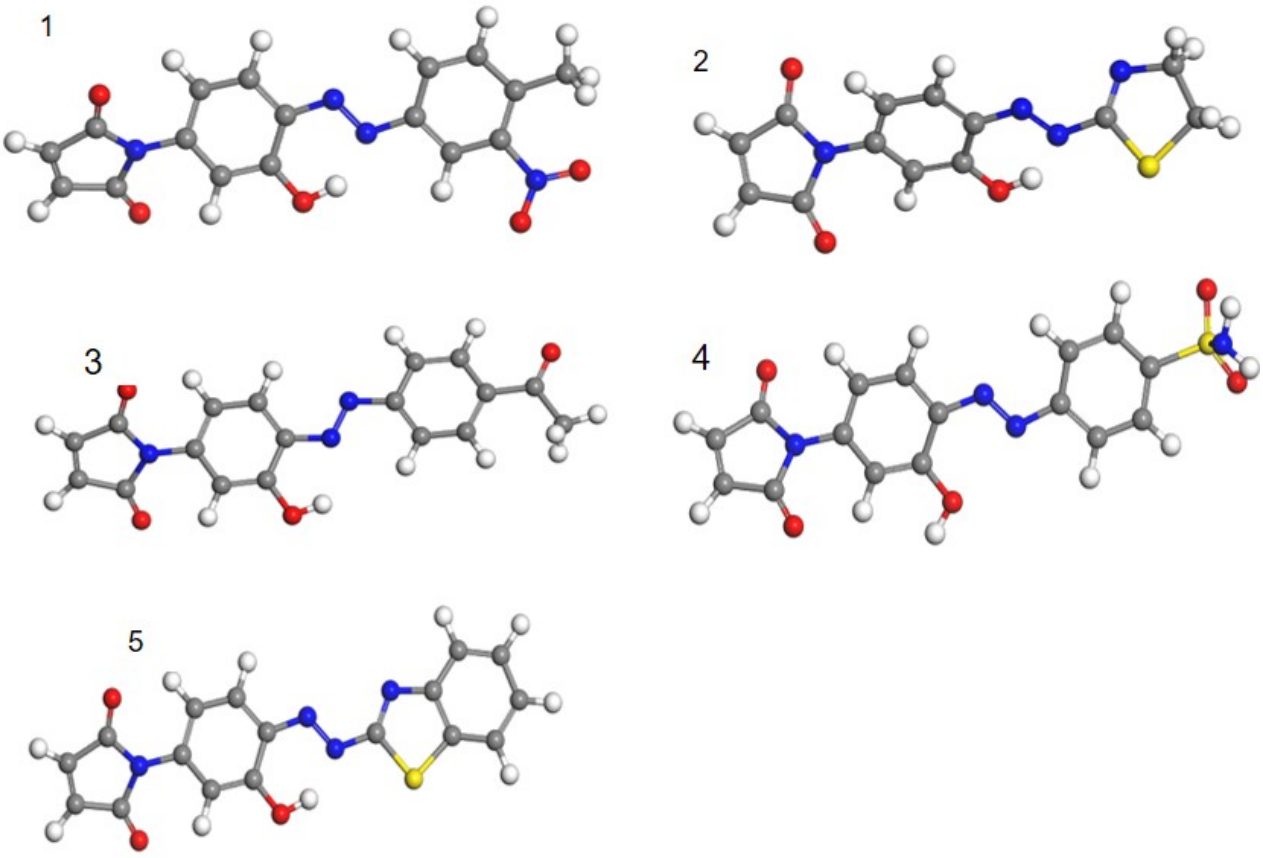

Figure 6. Optimization of Geometries and Structures of the Studied Molecules 1-5

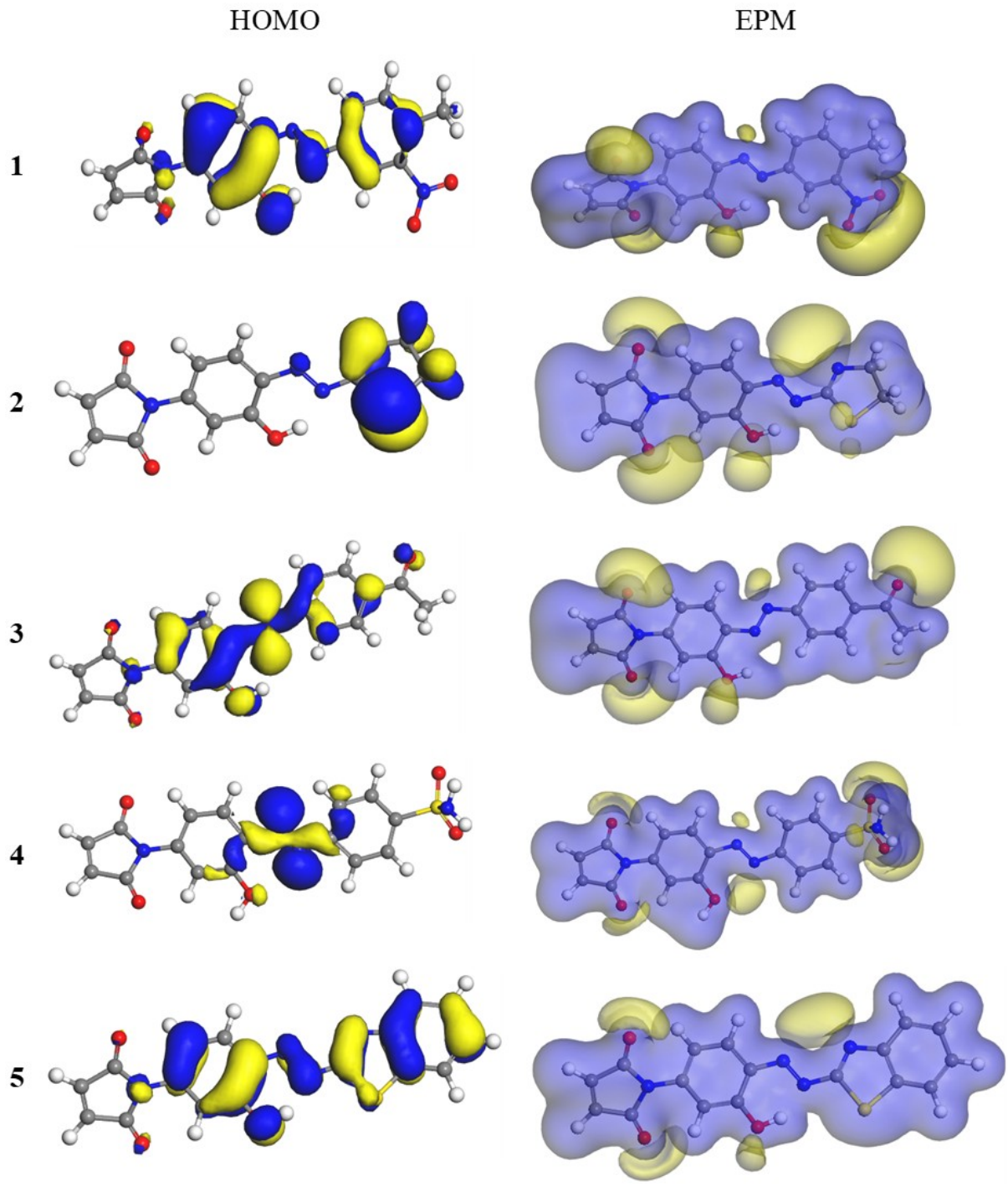

Figure 7. HOMO Orbitals Forms and Electrostatic Potential Map of the Studied Molecules

value of the HOMO-LUMO gap energy, high dipole moment, and good charge distribution of compound 1. Therefore, the aforementioned factors are responsible for its high antibacterial activity.

3.4 Molecular Docking Study

Molecular docking is an advanced computational method frequently used to predict binding orientations, energies, and key intermolecular forces in the binding of small molecules (ligands) to biological macromolecules (receptors) (Mutlaq et al.,

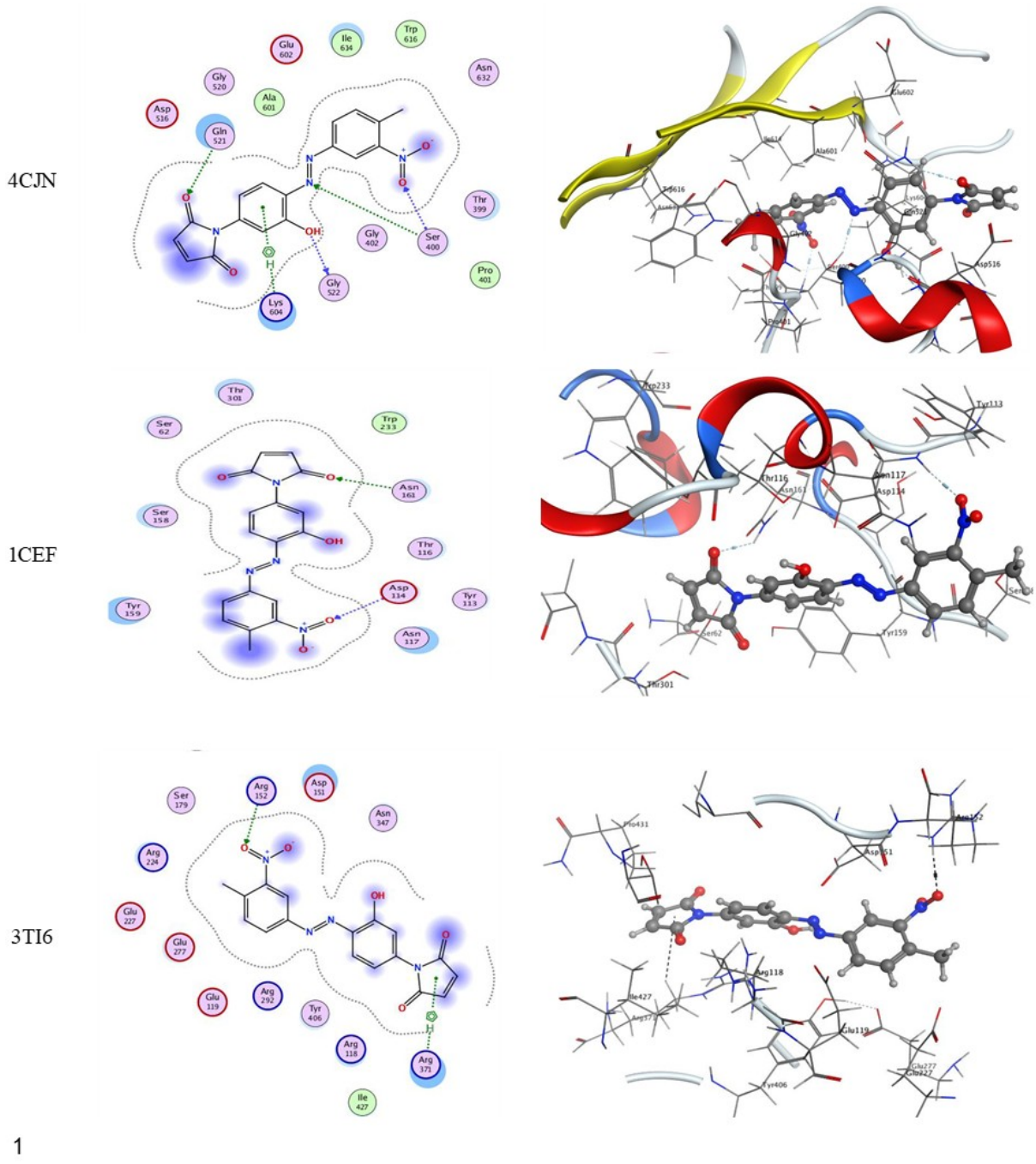

Figure 8. 2D and 3D Forms of Compound 1 with Target Proteins; 4CJN, 1CEF, and 3TI6

2021). The intensity and character of ligand-protein interactions are essential indicators of the biological activity of compound molecules as well as their capability to act as competent inhibitors of biological targets (Hamdani et al., 2020).

In the current project, the azo compound 1 was selected for molecular docking studies owing to its higher antibacterial activity. The docking of the molecule was performed against two penicillin-binding proteins (PBPs), named 4CJN and 1CEF, which are critical enzymes involved in the biosynthesis of the bacterial cell wall, as well as the viral enzyme neuraminidase (PDB ID: 3TI6), based on previously published literature (Ali et al., 2018). Based on the docking studies, Table 3 shows that compound 1 has the highest binding energy (-6.941 kcal/-mol) and RMSD of 1.780 for protein 4CJN, indicating that the docking pose is stable and optimal (Al-Salim and Al-Asadi, 2023).

Table 3. Molecular Docking Data of Compound 1 with Target 4CJN, 1CEF, and 3TI6

Proteins (Receptors)	RMSD	Affinity Energy (S) Kcal/mol	Interaction		
			Type	Amino Acid	Distance (Å)
4CJN	1.780	-6.941	H-donor	GLY 522	2.97
			H-acceptor	GLN 521	3.33
			H-acceptor	SER 400	3.16
			H-acceptor	SER 400	3.07
			pi-H	LYS 604	3.84
1CEF	0.827	-5.903	H-acceptor	ASN 161	3.05
			H-acceptor	ASP 114	3.12
3TI6	1.021	-5.916	H-acceptor	ARG 152	2.94
			pi-H	ARG 371	4.40

As can be observed in Figure 8, compound 1 binds to the 4CJN protein using various non-covalent bonding interactions. These noncovalent interactions involve hydrogen bonding between the oxygen and nitrogen atoms of ligand 1 and the relevant amino acid residues GLN-521, SER-400, and GLY-522 of the 4CJN protein, as well as a π-H bond between the aromatic ring of ligand 1 and LYS-604. This has been identified to play an essential role in the strength of ligand protein complexes (Al-Resayes et al., 2023; Falah Azeez et al., 2024).

Docking of compound 1 on the second penicillin-binding protein (PDB code: 1CEF) resulted in a binding energy of -5.903 kcal/mol with an RMSD of 0.827. As revealed in Figure 8, there are hydrogen-bond acceptor interactions of the ligand with ASN-161 and ASP-114, thus showing positive binding of the ligand in the active site but less than that of 4CJN (Osman, 2017; Prakash et al., 2021).

Further, docking analysis was performed on the neuraminid ase enzyme (PDB code: 3TI6). It showed moderate binding affinity with the following significant interactions: the hydrogen-bond acceptor type between the ligand's oxygen and ARG-152 and the π-H type between the aromatic ring and ARG-371. These results also imply antiviral activity for compound 1, but its most significant application is to bacterial targets. Overall, the molecular docking study provides strong theoretical evidence supporting the experimental findings on antibacterial activity. The favorable binding affinity of compound 1 for the penicillin-binding protein, together with multiple hydrogen bonds and π-H interactions, supports inhibition of bacterial cell wall biosynthesis as the mechanism of action. The high consistency among the docking scores, the DFT parameters, and the experimental in vitro antibacterial activity values confirms the validity of the study's strategy (Al-Resayes et al., 2023; Elsayed et al., 2023).

4. CONCLUSIONS

In this paper, a new set of heterocyclic azo compounds of N-(3-hydroxyphenyl) maleimide was designed and prepared, and a series of tests, including FT-IR, ^{1}H NMR, ^{13}C NMR, and MS spectroscopy, were conducted. The synthesized compounds exhibited potent inhibitory activity against *Staphylococcus aureus* and *Escherichia coli*, with compound 1 showing the most vigorous activity. The antibacterial activity was found to be related to the substituent effects and electronic properties, which were revealed by the density functional theory calculation, in that compound 1 had the lowest HOMO-LUMO energy gap value and the highest dipole moment value. The molecular docking results revealed that compound 1 exhibited a favorable binding mode to penicillin-binding protein 4CJN via hydrogen-bond interactions. Altogether, these findings suggest that the azo-maleimide derivatives, particularly compound 1, are promising scaffolds for new antibacterial agents and provide a foundation for further optimization.

5. ACKNOWLEDGMENT

The authors thank the Department of Chemistry within the College of Education for Pure Science at the University of Basra for their valuable support and guidance.

REFERENCES

Adu, J. K., C. D. K. Amengor, N. Mohammed Ibrahim, C. Amaning-Danquah, C. Owusu Ansah, D. D. Gbadago, and J. Sarpong-Agyapong (2020). Synthesis and in Vitro Antimicrobial and Anthelminthic Evaluation of Naphtholic and Phenolic Azo Dyes. *Journal of Tropical Medicine*, **2020**(1); 4850492

Al-Ameertaha, A. R. and R. H. Al-Asadi (2025). Design, Synthesis, Characterization, DFT, Molecular Docking Studies and Evaluation of Biological Activity of Benzamidethiourea Derivatives against HepG2 Hepatocellular Carcinoma Cell Lines. *Advanced Journal of Chemistry, Section A*, **8**(2); 220–244

Al-Asadi, R. H. (2019). Synthesis, DFT Calculation and Biological Activity of Some Organotellurium Compounds Containing Azomethine Group. *Orbital*, **11**(7); 402–410

Al-Asadi, R. H., M. K. Mohammed, and H. K. Dhaef (2020). Mercuration and Telluration of 2-Fluoro-5-nitroaniline: Synthesis, Antibacterial, and Computational Study. *Russian Journal of General Chemistry*, **90**(4); 703–709

Al-Resayes, S. I., A. J. Jarad, J. M. M. Al-Zinkee, T. H. Al-Noor, M. M. El-Ajaily, M. Abdalla, K. Min, M. Azam,

and R. K. Mohapatra (2023). Synthesis, Characterization, Antimicrobial Studies, and Molecular Docking Studies of Transition Metal Complexes Formed from a Benzothiazole-Based Azo Ligand. *Bulletin of the Chemical Society of Ethiopia*, **37**(4); 931–944

Al-Salim, Y. M. and R. H. Al-Asadi (2023). Synthesis, Anti-breast Cancer Activity, and Molecular Docking Studies of Thiourea Benzamide Derivatives and Their Complexes with Copper Ion. *Tropical Journal of Natural Product Research*, **7**(6); 3158–3167

Ali, Y., N. Muhamad Bunnori, D. Susanti, A. Muhammad Alhassan, and S. Abd Hamid (2018). Synthesis, In-Vitro and In Silico Studies of Azo-Based Calix[4]arenes as Antibacterial Agent and Neuraminidase Inhibitor: A New Look Into an Old Scaffold. *Frontiers in Chemistry*, **6**; 210

Dhaef, H. K., R. H. Al-Asadi, A. A. Shenta, and M. K. Mohammed (2021). Novel Bis Maleimide Derivatives Containing Azo Group: Synthesis, Corrosion Inhibition, and Theoretical Study. *Indonesian Journal of Chemistry*, **21**(5); 1212–1220

Elsayed, E. H., D. Al-Wahaib, A. E. D. Ali, B. A. Abd-El-Nabey, and H. A. Elbadawy (2023). Synthesis, Characterization, DNA Binding Interactions, DFT Calculations, and Covid-19 Molecular Docking of Novel Bioactive Copper(I) Complexes Developed via Unexpected Reduction of Azo-Hydrazo Ligands. *BMC Chemistry*, **17**(1); 159

Falah Azeez, Z., L. Ali Khaleel, and H. Ali Kadhim Kyhoiesh (2024). Synthesis, Biological Evaluation, Molecular Docking Analyses, and ADMET Study of Azo Derivatives Containing 1-Naphthol against MβL-Producing S. maltophilia. *Results in Chemistry*, **12**; 101864

Hamdani, S. S., B. A. Bhat, L. Tariq, S. I. Yaseen, I. Ara, B. Rafi, S. N. Hamdani, T. Hassan, and O. Rashid (2020). Antibiotic Resistance: The Future Disaster. *International Journal for Research in Applied Sciences and Biotechnology*, **7**; 101864

Irminova, S., B. Sezgin, and T. Tilki (2020). Novel Heterocyclic Azo Compounds: Synthesis, Characterization and DFT Calculations. *Süleyman Demirel Üniversitesi Fen Edebiyat Fakültesi Fen Dergisi*, **15**(2); 319–329

Jarallah, H. M., H. K. Dhaef, M. K. Mohammed, S. M. H. Ismal, and A. A. Hussein (2026). Synthesis, Characterization of Novel Azo Compounds as Corrosion Inhibitors for Carbon Steel in HCl, and Their Theoretical Study. *Science and Technology Indonesia*, **11**(1); 84–95

Jasim, E. Q., M. A. Muhammad-Ali, and A. Almakki (2023). Synthesis, Characterization, and Antibacterial Activity of Some Mesalazine Derivatives. *Science and Technology Indonesia*, **8**(3); 338–343

Marinescu, M., C. V. Popa, M. A. Tănase, A. C. Soare, C. Tablet, D. Bala, L. O. Cinteza, L. M. Diţu, I. C. Gifu, and C. Petcu (2022). Synthesis, Characterization, DFT Study and Antifungal Activities of Some Novel 2-(Phenyldiazenyl) Phenol Based Azo Dyes. *Materials*, **15**(22); 8162

Mohammed, M. K., F. A. Almasha, H. H. Al-Hujaj, R. H. Al-Asadi, H. A. Jaber, A. M. Jassem, and H. K. Dhaef (2024). Synthesis, Characterization, Cytotoxic Evaluation on MCF-7 Breast Cancer Cells, and Theoretical Studies of Novel 1,2,3-Triazoles. *Tropical Journal of Natural Product Research*, **8**(10); 8788–8795

Morrison, J. J., V. K. Brandt, and S. G. Yeates (2019). Comment on: Synthesis of New Azo Compounds Based on N-(4-Hydroxyphenyl)maleimide and N-(4-Methylphenyl)maleimide. *Molecules*, **24**(12); 2319

Mutlaq, D., A. Al-Shawi, and R. Al-Asadi (2021). Synthesis, Characterization, Anticancer Activity, and Molecular Docking of Novel Maleimide-Succinimide Derivatives. *Egyptian Pharmaceutical Journal*, **20**(4); 303–312

Osman, O. I. (2017). DFT Study of the Structure, Reactivity, Natural Bond Orbital and Hyperpolarizability of Thiazole Azo Dyes. *International Journal of Molecular Sciences*, **18**(2); 239

Piotto, S., S. Concilio, L. Sessa, R. Diana, G. Torrens, C. Juan, U. Caruso, and P. Iannelli (2017). Synthesis and Antimicrobial Studies of New Antibacterial Azo-Compounds Active against *Staphylococcus aureus* and *Listeria monocytogenes*. *Molecules*, **22**(8); 1372

Prakash, S., G. Somiya, N. Elavarasan, K. Subashini, S. Kanaga, R. Dhandapani, M. Sivanandam, P. Kumaradhas, C. Thirunavukkarasu, and V. Sujatha (2021). Synthesis and Characterization of Novel Bioactive Azo Compounds Fused with Benzothiazole and Their Versatile Biological Applications. *Journal of Molecular Structure*, **1224**; 129016

Rabel, M. and R. Prabhath (2015). A Study of the Structure-Property Relationship of Azole-Azine Based Homoleptic Platinum(II) Complexes and Tunability of the Photo-Physical Properties. University of Surrey (United Kingdom)

Scarim, C. B. and C. M. Chin (2021). The Use of Heterocyclic-Based Azo Compounds Bearing Pyrrolidine, Imidazole, Triazole, and Thiazole Moieties for the Treatment of Neglected Tropical Disease Caused by *Schistosoma mansoni*. *European Journal of Medicinal Chemistry Reports*, **1**; 100001

Shafeeq, A. A., Z. Mohammed, A. Hamandi, M. H. Mohammed, and G. Al-Shamma (2023). Synthesis, Characterization, and Antimicrobial Evaluation for New Azo-Linked Derivative of Heterocyclic Compounds. *Journal of Contemporary Medical Sciences*, **8**(1); 51–58

Temma, A. S., O. N. Ali, R. H. Al-Asadi, and M. K. Mohammed (2025). Evaluation of Schiff Bases Against Two Cancer Cell Lines: A Combined Experimental and Theoretical Approach. *Tropical Journal of Natural Product Research*, **9**(3); 967–972

Upadhayay, A., J. Ling, D. Pal, Y. Xie, F.-F. Ping, and A. Kumar (2023). Resistance-Proof Antimicrobial Drug Discovery to Combat Global Antimicrobial Resistance Threat. *Drug Resistance Updates*, **66**; 100890

Widjajanti, H., C. V. Handayani, and E. Nurnawati (2021). Antibacterial Activity of Endophytic Fungi from Sembukan (*Paederia foetida* L.) Leaves. *Science and Technology Indonesia*, **6**(3); 189–195

Wiegand, I., K. Hilpert, and R. E. W. Hancock (2008). Agar and Broth Dilution Methods to Determine the Minimal Inhibitory Concentration (MIC) of Antimicrobial Substances. *Nature Protocols*, **3**(2); 163–175

